

Crystal Structures and Magnetic Properties of Copper(II) Hexafluoroacetylacetonate Complexes with hnn and hin and Manganese(II) Hexafluoroacetylacetonate Complex with hin (hnn = 4,4,5,5-Tetramethylimidazolin-1-oxyl 3-Oxide; hin = 4,4,5,5-Tetramethylimidazolin-1-oxyl)

Tomoaki Ise, Takayuki Ishida,* and Takashi Nogami*

Department of Applied Physics and Chemistry, The University of Electro-Communications, Chofu, Tokyo 182-8585

(Received June 14, 2002)

We report here the structures and magnetic properties of hnn and hin complexes with copper(II) and manganese(II) hexafluoroacetylacetonates, [{Cu(hfac)$_2$(H$_2$O)}$_2$(μ-hnn)] (**1**), [Cu(hfac)$_2$(hin)$_2$] (**2**), and [Mn(hfac)$_2$(hin)$_2$] (**3**). X-ray crystallographic analysis of **1** revealed that **1** was a dinuclear complex containing an hnn bridge. Magnetic measurements of **1** indicate the presence of intramolecular ferromagnetic coupling between copper and radical spins. The data were analyzed as a metal-radical-metal three-spin system, giving $2J/k = +16.2$ K ($H = -2J(S_1S_2 + S_2S_3)$). The ferromagnetic interaction can be explained in terms of the axial coordination of the hnn nitrogen to Cu(II). Complexes **2** and **3** were revealed to be isomorphous mononuclear complexes possessing two hin ligands. Although the molecules have a radical-metal-radical system, the magnetic data of **3** could not be analysed only with intramolecular interactions. Strong intermolecular antiferromagnetic interactions ($2|J|/k \gg 300$ K) were suggested among the hin ligands because the interatomic O···N distances (2.41–2.51 Å) were shorter than the sum of the van der Waals radii for **2** and **3**. These strong interactions are successfully introduced to metal-radical hybrid systems owing to the choice of small ligands, although the complexes do not possess polymeric networks.

There have been a number of hybrid-complexes which have flexible functionality of organic materials and strong magnetic interactions between metal ions and radicals.[1] The design of magnetic materials with a high bulk ferromagnetic or ferrimagnetic transition temperature, T_c, is one of the main challenges in this field. T_c is well known to be strongly dependent on the magnitude of the exchange interaction between the spin sources.[2] We assume that the choice of small ligands and anions is crucial in order to bestow strong exchange interaction on magnetic materials. We chose 4,4,5,5-tetramethylimidazolin-1-oxyl 3-oxide (hnn) and 4,4,5,5-tetramethylimidazolin-1-oxyl (hin) as ligands (Chart 1). These are the smallest derivatives in the nitronylnitroxide and iminonitroxide families.[3] These radicals can bridge paramagnetic metal ions through the O–N–C–N–O or O–N–C–N π-electron systems. Although the isolation of hin was claimed to be difficult because of its instability,[3] complexation affords a chance to purify and characterize hin compounds. Stabilization by complex formation is widely utilized for preparation of compounds of low-valent main group elements.[4] We have reported a practically diamagnetic hin complex, [CdCl$_2$(hin)$_4$], owing to extraordinarily strong intermolecular antiferromagnetic coupling.[5] We report here the X-ray crystal structures and magnetic properties of the hnn and hin complexes with paramagnetic [Cu(hfac)$_2$] (hfac = 1,1,1,5,5,5-hexafluoropentane-2,4-dionate). We also report structures and magnetic properties of the isomorphous hin complex with Mn(hfac)$_2$ in order to elucidate magnetic exchange pathways.

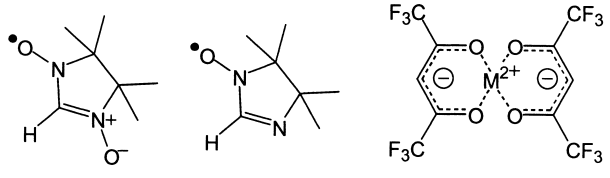

Chart 1.

Experimental

Materials. 4,4,5,5-Tetramethylimidazolin-1-oxyl 3-Oxide (hnn) was prepared according to the procedure previously reported.[3] 4,4,5,5-Tetramethylimidazolin-1-oxyl (hin) was prepared according to the literature method[3] with a slight modification.

4,4,5,5-Tetramethylimidazolin-1-oxyl (hin): Solutions of hnn (1.0 g, 6.4 mmol) in CH_2Cl_2 (5 mL) was added to a suspension of $NaNO_2$ (1.1 g, 16 mmol) in CH_2Cl_2 (30 mL) and CH_3CO_2H (3.5 mL, 61 mmol). The reaction mixture was stirred for 5 min to give a bright orange solution. After filtration and neutralization with aqueous $NaHCO_3$, the organic layer was washed with water, and the aqueous phase was extracted with CH_2Cl_2 (100 mL). The combined organic phase was dried over $MgSO_4$. The solution was concentrated and chromatographed over a short column (silica gel). Elution with a solution of CH_2Cl_2/diethyl

ether (4/1 in volume) followed by removal of the solvent in vacuo gave a pure orange product of 680 mg (75%).

[{Cu(hfac)$_2$(H$_2$O)}$_2$(μ-hnn)] (1): Solutions of hnn (100 mg, 0.64 mmol) in CH_2Cl_2 (7.0 mL) and of Cu(hfac)$_2$ (302 mg, 0.64 mmol) in CH_2Cl_2 (2.0 mL) were mixed, the combined solution was allowed to stand in a cool and dark place for 2 days, and dark-red crystals of **1** were precipitated.

[Cu(hfac)$_2$(hin)$_2$] (2): Solutions of hin (200 mg, 1.42 mmol) in dry diethyl ether (0.8 mL) and of Cu(hfac)$_2$ (339 mg, 0.71 mmol) in dry diethyl ether (0.5 mL) were mixed, the combined solution was allowed to stand in a cool and dark place for 1 day, and dark-brown crystals of **2** were precipitated.

[Mn(hfac)$_2$(hin)$_2$] (3): Solutions of hin (100 mg, 0.71 mmol) in dry diethyl ether (0.2 mL) and of dehydrated Mn(hfac)$_2$ (333 mg, 0.71 mmol) in dry ether (0.2 mL) were mixed, the combined solution was allowed to stand in a cool and dark place for one day, and dark-brown crystals of **3** were precipitated.

The isolated hnn, [{Cu(hfac)$_2$(H$_2$O)}$_2$(μ-hnn)], [Cu(hfac)$_2$-(hin)$_2$] and [Mn(hfac)$_2$(hin)$_2$] could be stored at -20 °C for several months, but isolated hin completely decomposed upon standing overnight at room temperature.

Elemental analysis (C, H, N) of these complexes on a Fisons EA-1108 by a usual combustion method revealed that the metal/radical ratios are 2/1, 1/2, and 1/2 for **1**, **2**, and **3**, respectively. Anal. Calcd. for $C_{27}H_{21}N_2O_{12}F_{24}Cu_2$ (**1**): C, 28.27; H, 1.84; N, 2.43%. Found: C, 28.45; H, 1.95; N, 2.85%. Calcd. for $C_{24}H_{28}N_4O_6F_{12}Cu_1$ (**2**): C, 37.73; H, 3.27; N, 7.13%. Found: C, 37.93; H, 3.71; N, 7.37%. Calcd. for $C_{24}H_{28}N_4O_6F_{12}Mn_1$ (**3**): C, 38.36; H, 3.76; N, 7.46%. Found: C, 38.66; H, 3.57; N, 7.59%.

X-ray Crystallographic Analysis. X-ray diffraction data were collected on a Rigaku Raxis-Rapid IP diffractometer with graphite monochromated Mo $K\alpha$ radiation (λ = 0.71069 Å) at 90.2 or 153 K. The structures were directly solved by a heavy-atom Patterson method in the teXsan program package.[6] Numerical absorption correction was used. Full-matrix least-squares methods were applied using all of the unique diffraction data.[7] A trifluoromethyl group C(11) of **1** was solved to be disordered into two conformations with a 1/1 population, leading to a considerable improvement in the refinement for **1**. The thermal displacement parameters of non-hydrogen atoms were anisotropically refined, but the positional and isotropic thermal parameters of hydrogen atoms were not refined. For **2** and **3**, all of the trifluoromethyl groups were solved in a disordered model. All of the hydrogen atoms could be found in difference Fourier maps, and the parameters of the hydrogen atoms were included in the refinement. The R_1 value of **3** was 0.081 because of the large thermal anisotropy of fluorine atoms, although other atoms could be satisfactorily refined.

Magnetic Measurements. Magnetic susceptibility was measured on a Quantum Design MPMS SQUID magnetometer equipped with a 7 T coil in a temperature range down to 1.8 K. The magnetic responses were corrected with diamagnetic blank data of the sample holder, obtained separately. The diamagnetic contribution of the sample itself was estimated from Pascal's constant.

Results and Discussion

X-ray Crystal Structure Analysis. Table 1 summarizes the X-ray crystallographic data for [{Cu(hfac)$_2$(H$_2$O)}$_2$(μ-hnn)] (**1**), [Cu(hfac)$_2$(hin)$_2$] (**2**), and [Mn(hfac)$_2$(hin)$_2$] (**3**). Figure 1 shows the molecular structure of **1**, which reveales a dinuclear complex involving an hnn bridge. One Cu(hfac)$_2$·H$_2$O and a half of hnn are crystallographically independent. The central hnn ligand is sandwitched by two copper ions, forming a linear three-spin system. The copper ions are coordinated by four oxygens of two hfac ligands occupying the equatorial positions. One oxygen of hnn and H$_2$O are coordinated at the axial position. Selected bond distances and angles are given in Table 2. The octahedra of both copper centers are severely distorted with the axial Cu(1)–O(5) and Cu(1)–O(6) bonds much longer than the equatorial ones: 2.46(2) and 2.25(8) Å vs 1.94(9), 1.93(4), 1.94(2) and 1.96(1) Å. An axial site of Cu is capped by oxygen atom of H$_2$O, which prevents the formation of a polymeric network in the crystal. This complex is expected to show intramolecular ferromagnetic interaction, i.e., the molecule has a ground quartet state, because this coordination type is essentially the same as that of [Cu(hfac)$_2$NN–Me] (NN–Me = 2,4,4,5,5–pentamethylimidazoline-1-oxyl 3-oxide), which shows ferromagnetic interaction between the Cu ion and radical spin.[8] This ferromagnetic interaction can be explained in terms of orbital orthogonality between the copper $3d_{x^2-y^2}$ and the nitrogen $2p_z$ orbitals, since the

Table 1. Selected X-ray Crystallographic Data of **1**, **2** and **3**

Compound	**1**	**2**	**3**
Formula	$C_{27}H_{21}N_2O_{12}F_{24}Cu_2$	$C_{24}H_{28}N_4O_6F_{12}Cu$	$C_{24}H_{28}N_4O_6F_{12}Mn$
Mol wt	1148.52	760.03	751.42
Crystal system	Orthombic	Triclinic	Triclinic
Space group	*Fdd*2	$P\bar{1}$	$P\bar{1}$
a/Å	35.607(7)	11.088(1)	10.985(5)
b/Å	13.173(9)	16.871(5)	17.153(3)
c/Å	17.094(1)	10.061(1)	9.778(3)
α/ degree		105.50(1)	105.18(5)
β/ degree		111.66(4)	110.59(4)
γ/ degree		72.14(8)	75.21(7)
V/Å^3	8018.66(4)	1634.25(5)	1637.29(6)
Z	8	2	2
D_{calc}/ g cm^{-3}	1.90	1.54	1.52
T/K	90.2	90.2	153
$R(I > 2\sigma(I))$	0.038	0.051	0.081

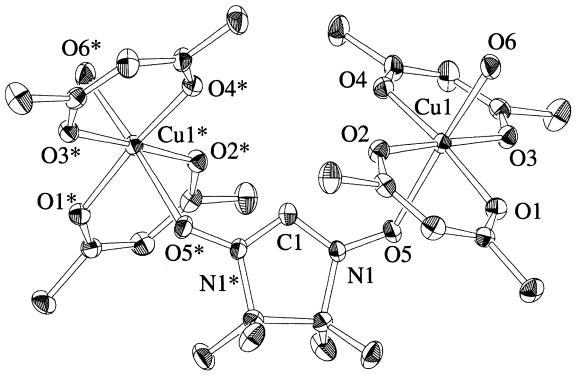

Fig. 1. ORTEP view of [{Cu(hfac)$_2$(H$_2$O)}$_2$(μ-hnn)] at the 50% probability level. The fluorine and hydrogen atoms are omitted for the sake of clarity. Symmetry opetration code for* is $-x + 3/2, -y + 1/2, z$.

Table 2. Selected Bond Distances (Å) and Angles (Degree) for [{Cu(hfac)$_2$(H$_2$O)}$_2$(μ-hnn)] (**1**)

Cu(1)–O(1)	1.949(2)	Cu(1)–O(4)	1.961(2)
Cu(1)–O(2)	1.934(2)	Cu(1)–O(5)	2.462(2)
Cu(1)–O(3)	1.940(2)	Cu(1)–O(6)	2.258(2)
N(1)–C(1)	1.323(7)	O(5)–N(1)	1.285(3)
O(1)–Cu(1)–O(2)	92.84(9)	O(1)–Cu(1)–O(3)	85.36(9)
O(1)–Cu(1)–O(4)	170.6(1)	O(1)–Cu(1)–O(5)	85.70(8)
O(1)–Cu(1)–O(6)	90.72(9)	O(2)–Cu(1)–O(3)	178.20(9)
O(2)–Cu(1)–O(4)	89.14(9)	O(2)–Cu(1)–O(5)	90.05(8)
O(2)–Cu(1)–O(6)	88.98(9)	O(3)–Cu(1)–O(4)	92.65(9)
O(3)–Cu(1)–O(5)	90.97(9)	O(3)–Cu(1)–O(6)	90.97(9)
O(4)–Cu(1)–O(5)	85.11(8)	O(4)–Cu(1)–O(6)	98.51(9)
O(5)–Cu(1)–O(6)	176.24(9)		

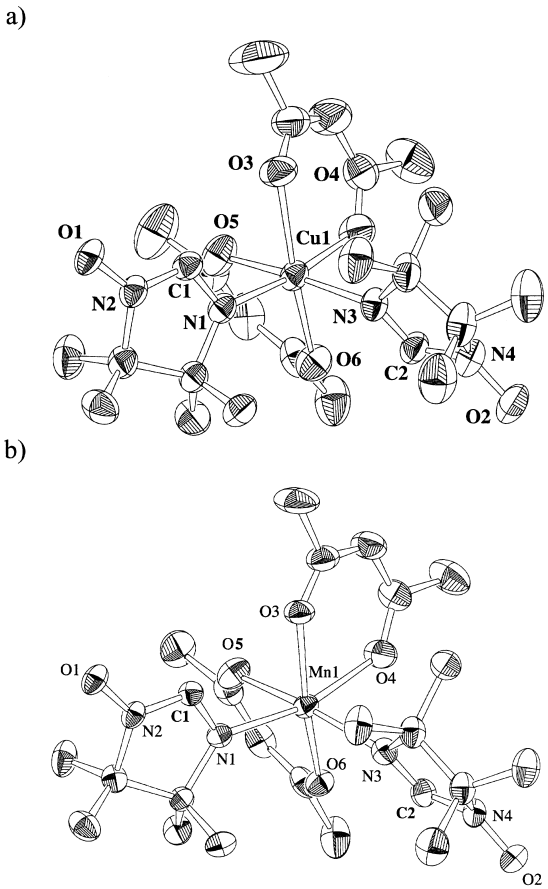

Fig. 2. ORTEP drawings of [Cu(hfac)$_2$(hin)$_2$] (a) and [Mn(hfac)$_2$(hin)$_2$] (b) at the 50% probability level. The fluorine and hydrogen atoms are omitted for the sake of clarity.

nitroxide oxygen atom is coordinated at an axial site of the copper ion.

Figure 2(a) shows that **2** is a mononuclear complex. The copper atoms are octahedrally coordinated by two oxygens of two hfac ligands and two nitrogens of hin. The interatomic bond distances of N(1)–C(1), N(2)–C(1) and O(1)–N(2) are close to the corresponding distances in other iminonitroxide radical derivatives.[9] Two oxygens of two hfac ligands are coordinated at the axial position. Selected bond distances and angles are given in Table 3 (M = Cu). The imino nitrogen atom coordinates to the Cu ion, whereas the nitroxide oxygen atom remains uncoordinated in spite of the potential coordination ability of nitroxide oxygen atoms. The strong coordination ability of the imino nitrogen atoms can be understood in view of the steric congestion around imino nitrogen and nitroxide oxygen atoms. This complex is expected to show intramolecular antiferromagnetic interaction because the hin nitrogen atom coordinates to an equatorial site of the Cu ion, in contrast to the hnn oxygen atoms occupying axial positions of the Cu ion in **1**.

In order to compare the structures and magnetic properties of other metal derivatives, we also prepared complexes consisting of hin and Mn(hfac)$_2$. Figure 2(b) shows that **3** is a mononuclear complex which an isomorphous structure of **2**. Selected bond distances and angles are given in Table 3 (M = Mn). The molecular arrangements of **2** and **3** are also quite similar.

Compounds **2** and **3** do not form any polymeric network in the crystals. However, as Fig. 3 shows, short intermolecular distances of 2.45(2) Å (O(1)···N(2*)) and 2.50(6) Å (O(2)···N(4#)) were found in **2**, and 2.41(3) Å (O(1)···N(2*)) and 2.42(1) Å (O(2)···N(4#)) in **3**, where* and # denote symmetry operation codes of $1-x, 1-y, 1-z$ and $-x, -y, -z$, respectively. These distances are much shorter than the sum of the van der Waals radii of oxygen and nitrogen (3.07 Å).[10] We assumed that hin groups formed an intermolecular dimer of nitroxide groups. The intermolecular magnetic interactions in **2** and **3** are expected to be antiferromagnetic because of the orbital overlap between adjacent magnetic orbitals.

Magnetic Properties. Magnetic susceptibility χ_m of **1** was measured in the temperature range 1.8–100 K, and the plot of $\chi_m T$ vs temperature is shown in Fig. 4. At 100 K, the $\chi_m T$ value for **1** is 1.3 cm^3 mol^{-1} K. Upon cooling, $\chi_m T$ increased to the maximum value (1.92 cm^3 mol^{-1} K) at 5 K, and then decreased. This magnetic behavior indicates that intramolecular ferromagnetic interaction is operative for **1**, together with a slight intermolecular antiferromagnetic interaction. We attempted to fit the result of the magnetic measurements by using the linear three spins system of $S = 1/2$ model given by Eq. 1,[11] based on the spin Hamiltonian $H = -2J(S_1 \cdot S_2 + S_2 \cdot S_3)$ with a Weiss constant θ, where all symbols have their usual

Table 3. Selected Bond Distances (Å) and Angles (Degree) for $[M(hfac)_2(hin)_2]$

	M = Cu	M = Mn
M(1)–O(3)	2.262(2)	2.148(2)
M(1)–O(4)	2.001(2)	2.174(2)
M(1)–O(5)	2.004(2)	2.177(2)
M(1)–O(6)	2.349(2)	2.163(2)
M(1)–N(1)	2.036(2)	2.224(3)
M(1)–N(3)	2.032(2)	2.208(3)
N(1)–C(1)	1.276(4)	1.279(3)
N(2)–C(1)	1.369(4)	1.375(3)
O(1)–N(2)	1.267(3)	1.264(3)
N(3)–C(2)	1.284(4)	1.283(3)
N(4)–C(2)	1.384(4)	1.374(3)
O(2)–N(4)	1.271(4)	1.259(3)
O(3)–M(1)–O(4)	84.05(8)	81.29(7)
O(3)–M(1)–O(5)	85.52(8)	89.62(8)
O(3)–M(1)–O(6)	159.49(8)	163.28(8)
O(3)–M(1)–N(1)	89.19(8)	86.72(8)
O(3)–M(1)–N(3)	100.85(8)	99.51(8)
O(4)–M(1)–O(5)	89.92(9)	89.03(8)
O(4)–M(1)–O(6)	79.09(8)	84.47(7)
O(4)–M(1)–N(1)	171.77(8)	166.45(8)
O(4)–M(1)–N(3)	87.18(9)	88.47(8)
O(5)–M(1)–O(6)	82.90(8)	81.40(7)
O(5)–M(1)–N(1)	84.87(8)	84.59(8)
O(5)–M(1)–N(3)	172.67(8)	170.05(8)
O(6)–M(1)–N(1)	106.50(8)	106.29(8)
O(6)–M(1)–N(3)	89.95(8)	88.78(7)
N(1)–M(1)–N(3)	98.74(8)	99.77(8)

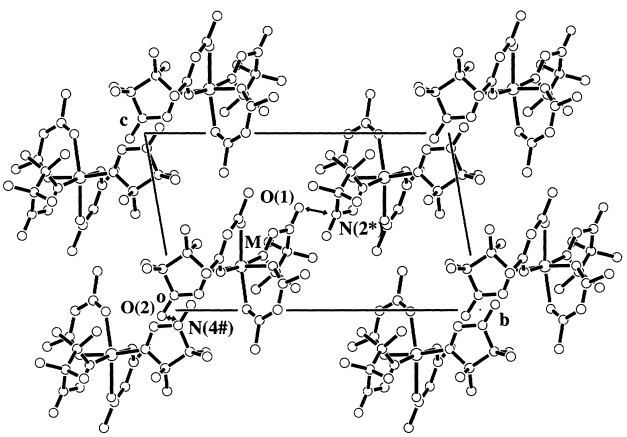

Fig. 3. Intermolecular short distances in the crystals of $[M(hfac)_2(hin)_2]$. Selected interatomic distances are: $d(O(1)\cdots N(2^*))$ = 2.45(2) and $d(O(2)\cdots N(4\#))$ = 2.50(6) Å for M = Cu. $d(O(1)\cdots N(2^*))$ = 2.41(3) and $d(O(2)\cdots N(4\#))$ = 2.42(1) Å for M = Mn. Symmetry operation codes : *: $1-x, 1-y, 1-z$; #: $-x, -y, -z$.

meaning. The exchange parameter J is the spin-spin coupling constant between Cu ions and radical. The best fit parameters of g, $2J/k$, and θ values are 2.068, +16.2 K, and −0.2 K respectively. The $2J/k$ value for **1** is slightly smaller than that for $[Cu(hfac)_2NN–Me]$ (+18.5 K).[8]

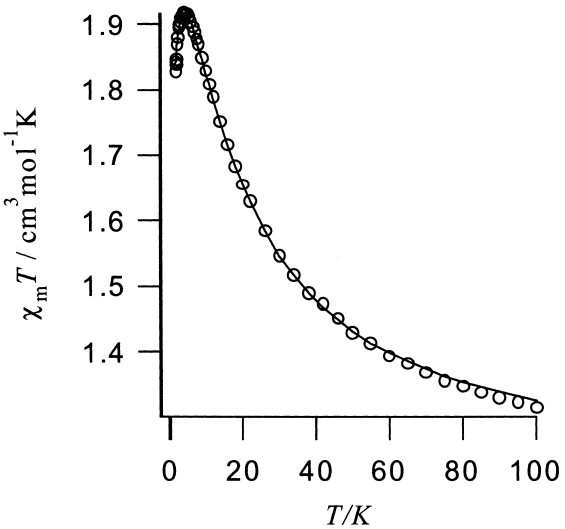

Fig. 4. Temperature dependence of the product $\chi_m T$ of $[\{Cu(hfac)_2(H_2O)\}_2(\mu\text{-hnn})]$ (○). Solid line corresponds to the theoretical curve, parameters of which are given in the text.

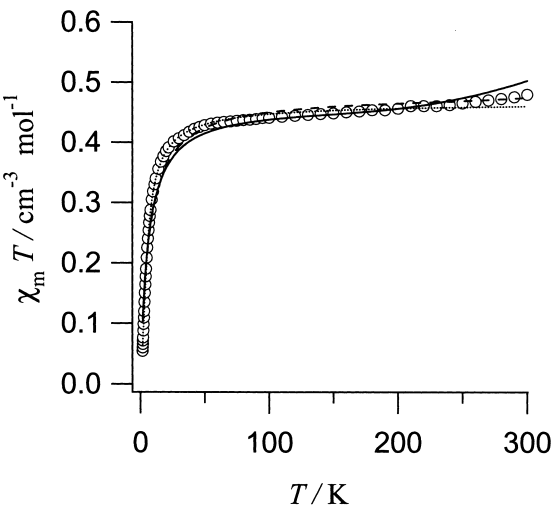

Fig. 5. Temperature dependence of the product $\chi_m T$ of $[Cu(hfac)_2(hin)_2]$ (○), compared with the theoretical curves based on Eq. 1 (—), Eq. 2 (- - -) and Eq. 4 (···), respectively.

$$\chi = \frac{Ng^2\mu_B{}^2}{4k(T-\theta)} \frac{10 + \exp(-J/kT) + \exp(-3J/kT)}{2 + \exp(-J/kT) + \exp(-3J/kT)} \quad (1)$$

The plot of $\chi_m T$ vs temperature of **2** is shown in Fig. 5. At room temperature, the $\chi_m T$ value, 0.48 cm^3 mol^{-1} K, is lower than the expected value of three S = 1/2 spin (1.125 cm^3 mol^{-1} K). This result indicates that a large intra- or intermolecular antiferromagnetic interaction is operative in **2** at this temperature. The above structural analysis of **2** showed that hin moieties formed a dimer. In this case, there are two conceivable models. One is a doublet/quartet model with a Weiss constant (Eq. 1),[11] on the basis of three-spin systems which is similar to the case of **1**. We assume here that the exchange in-

teraction between Cu-hin is larger than that between the through-space hin···hin dimer. The best fit parameters of g, $2J/k$, and θ values are 2.23, −425 K, and −5.9 K, respectively.

The other model is a combined singlet/triplet + doublet model with a Weiss constant (Eq. 2). We assume that the exchange interaction within the hin···hin dimer is larger than that of Cu-hin and that the second term of Eq. 2 implies a Curie spin from the copper ion ($S = 1/2$). The exchange parameter J is the spin-spin coupling constant between radical dimers, and θ is among Cu ions. The best fit parameters of the g, $2J/k$, and θ values are 2.26, −998 K, and −6.7 K, respectively.

$$\chi = \frac{2Ng^2\mu_B{}^2}{kT}\frac{1}{3+\exp(-2J/kT)} + \frac{Ng^2\mu_B{}^2S(S+1)}{3k(T-\theta)} \quad (2)$$

For further discussion about exchange pathways in the crystal of **2**, especially which model described above is more reliable, the following experimental results give valuable information. We prepared the manganese derivative (**3**) according to the same synthetic procedure as that of **2** and revealed that the molecular and crystal structures of **3** were essentially the same as those of **2**. We analyzed magnetic data of **3** based on the same magnetic coupling model with different spin quantum number of the metal ion. The plot of χ_mT vs temperature of **3** is shown in Fig. 6. At room temperature, the χ_mT value, 4.41 cm^3 mol^{-1} K, is lower than the expected value of the sum of two $S = 1/2$ and one $S = 5/2$ spins (5.125 cm^3 mol^{-1} K). This result indicates that a large intra- or intermolecular antiferromagnetic interaction is operative in **3** at this temperature, like the case of **2**. On cooling, the χ_mT value decreases and reaches a plateau (about 4.3 cm^3 mol^{-1} K) in a temperature range 250–140 K. This plateau is consistent with a paramagnetic Mn ion (4.375 cm^3 mol^{-1} K). The above structural analysis of **3** showed that hin moieties formed a dimer. Thus, we can propose that very strong antiferromagnetic interactions operate in an hin dimer in the crystal at this temperature range, and that the magnetic moments of hin are completely canceled. We attempted to fit the result of the magnetic measurements by using a combined dimer model given by Eq. 2 with $S = 5/2$. The exchange parameter J is the spin–spin coupling constants between radical dimer, θ is between Mn ions. The best fit parameters of the g, $2J/k$, and θ values are 2.04, −3840 K, and −6.2 K, respectively. Because of a slight temperature dependence of χ_mT up to 300 K, the estimated J value does not have sufficient accuracy, but we can conclude that $J/k \gg 300$ K.

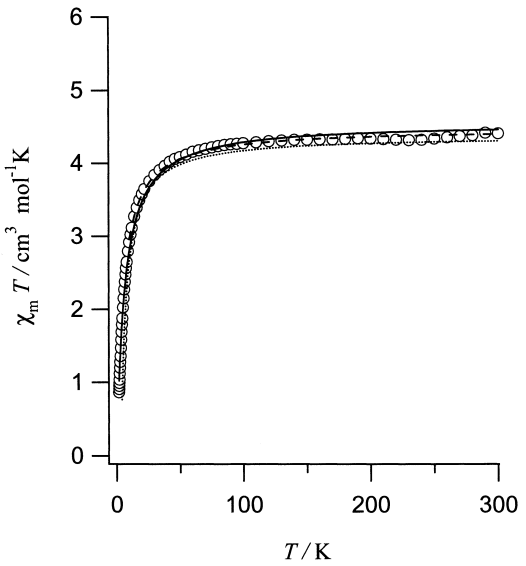

Fig. 6. Temperature dependence of the product χ_mT of [Mn(hfac)$_2$(hin)$_2$] (○), compared with the theoretical curves based on Eq. 2 (—), Eq. 3 (- - -) and Eq. 5 (···), respectively.

On the other hand, assuming that the magnitude of intramolecular interaction is larger than that of intermolecular interaction, antiferromagnetic interaction between an Mn ion ($S = 5/2$) and two hin ($S = 1/2$) must be operative. We attempted to fit the result of the magnetic measurements by using a linear-arrayed model of $S = 1/2$, 5/2, and 1/2 given by Eq. 3.[12]

$$\chi = \frac{Ng^2\mu_B{}^2}{12(T-\theta)}\frac{30\exp A + 105\exp B + 252\exp C + 105}{2\exp A + 3\exp B + 4\exp C + 3} \quad (3)$$

$$A = \frac{-7J}{kT}\ ,\ B = \frac{-2J}{kT}\ ,\ \text{and}\ C = \frac{5J}{kT}\ .$$

The exchange parameter J is ascribable to the spin-spin coupling constants between Mn ion and radicals, and θ is among molecules. The best fit parameters of g, $2J/k$, and θ values are 3.09, −994 K, and −5.1 K, respectively. This g value is not acceptable for Mn ions, and consequently this model should be abandoned.

Therefore, it seems reasonable to conclude that the magnitude of intermolecular through-space interaction is larger than that of intramolecular through-bond interaction in the case of **2** and **3**. Furthermore, the intermolecular interactions are much larger than 300 K. These results indicate that the hin ligands can be useful for achieving the strong intermolecular exchange interaction.

Assuming that both **2** and **3** can be regarded as chains of the Cu and Mn ions, respectively, with intervening hin pairs, we attempted to fit the result of the magnetic measurements of **2** and **3** by using chain models of $S = 1/2$ given by Eq. 4[13] and $S = 5/2$ given by Eq. 5,[14] based on the spin Hamiltonian $H = -2J\,\Sigma S_i{\cdot}S_{i+1}$, respectively. The calculated curves are superposed in Figs. 5 and 6. The exchange parameter J is ascribable to the spin-spin coupling constant between the metal ions in the chain. The best fit parameters of g and $2J/k$ are 2.23 and −13 K for **2** and 2.00 and −1.6 K for **3**, respectively. These chain models are good fits for both cases of **2** and **3**. This result indicates that the magnitude of the antiferromagnetic interaction is as large as a chemical bond, and that the hin pair plays a role of an antiferromagnetic coupler.

$$\chi = \frac{Ng^2\mu_B{}^2}{k}\frac{0.25 + 0.074975x + 0.075235x^2}{1.0 + 0.9913x + 0.172135x^2 + 0.757825x^3} \qquad x = \frac{|J|}{2kT} \quad (4)$$

$$\chi = \frac{35Ng^2\mu_B{}^2}{12k}\frac{1+u}{1-u} \qquad u = \coth\left[\frac{35J}{8kT}\right] - \left[\frac{8kT}{35J}\right] \quad (5)$$

We have demonstrated the preparation and full characterization of [{Cu(hfac)$_2$(H$_2$O)}$_2$(μ-hnn)] and [Cu(hfac)$_2$(hin)$_2$]. The different exchange interactions of **1** and **2** are due to different coordination geometries of ligand molecules to Cu ion. This result indicates that the choice of a small ligand is effective to bestow strong exchange interaction. Recently Gateschi and co-workers reported that polymeric metal hexafluoroacetylacetonate-nitronylnitroxide systems were potentially good candidates for single-molecule magnets.[15] Complexes **1**, **2**, and **3** can be regarded as prototypes of possible polymeric forms when possible intrachain ferro- or ferrimagnetic coupling take place rather than antiferromagnetic hin···hin coupling. Preparation of polymeric complexes using hin and hnn with other large anisotropically metal ions such as Co(II) ions is currently underway.

This work was supported by Grants-in-Aid for Scientific Research on Priority Areas (No. 730/11224204 and 401/11136212) from the Ministry of Education, Culture, Sports, Science and Technology.

References

1 A. Caneschi, D. Gatteschi, and R. Sessoli, *Acc. Chem. Res.*, **22**, 392 (1989); A. Caneschi, D. Gatteschi, and P. Rey, *Prog. Inorg. Chem.*, **39**, 331 (1991).

2 O. Kahn, "Molecular Magnetism", VHC, New York (1993).

3 E. F. Ullman, L. Call, and J. H. Osiecki, *J. Org. Chem.*, **35**, 3623 (1970).

4 For example, W. E. Buhro, A. T. Patton, C. E. Strouse, and J. A. Gladysz, *J. Am. Chem. Soc.*, **105**, 1056 (1983).

5 T. Ise, T. Ishida, and T. Nogami, *Mol. Cryst. Liq. Cryst.*, **379**, 147 (2002).

6 "*teXsan*: crystal structure analysis package," Molecular Structure Corp., The Woodland, TX (1985, 1999).

7 The CIF data for the three crystals are deposited as Document No. 75052 at the Office of the Editor of Bull. Chem. Soc. Jpn. Crystallographic data have been deposited at the CCDC, 12 Union Road, Cambridge CBZ IEZ, UK and copies can be obtained on request, free of charge, by quoting the publication and the deposition numbers 187504–187506 for **1**–**3**.

8 A. Caneschi, D. Gatteschi, J. Laugier, and P. Rey, *J. Am. Chem. Soc.*, **109**, 2191 (1987).

9 For example, H. Oshio, T. Watanabe, A. Ohto, T. Ito, and H. Masuda, *Inorg. Chem*, **35**, 472 (1996).

10 A. Bondi, *J. Phys. Chem.*, **68**, 441 (1964).

11 N. Tyutyulkov and C. S. Karabunarliev, *Int. J. Quantum Chem*, **29**, 1325 (1986).

12 M. Kitano, Y. Ishimaru, K. Inoue, N. Koga, and H. Iwamura, *Inorg. Chem*, **33**, 6012 (1994).

13 J. C. Bonner and M. E. Fisher, *Phys. Rev. A*, **135**, 640 (1964).

14 M. E. Fisher, *Am. J. Phys.*, **32**, 343 (1964).

15 A. Caneschi, D. Gatteschi, N. Lalioti, C. Sangregorio, R. Sessoli, G. Venturi, A. Vindigni, A. Rettori, M. G. Pini, and M. A. Novak, *Angew. Chem,. Int, Ed.*, **40**, 1760 (2001).